AUTHOR(S): CHITRA DEVI, M., RAJENDRAN, L., BIN YOUSAF, A. and FERNANDEZ, C.

TITLE: Non-linear differential equations and rotating disc electrodes: Padé approximation technique.

YEAR: 2017

Publisher citation: CHITRA DEVI, M., RAJENDRAN, L., BIN YOUSAF, A. and FERNANDEZ, C. 2017. Non-linear differential equations and rotating disc electrodes: Padé approximation technique. Electrochimica acta [online], 243, pages 1-6. Available from: https://doi.org/10.1016/j.electacta.2017.05.061

OpenAIR citation: CHITRA DEVI, M., RAJENDRAN, L., BIN YOUSAF, A. and FERNANDEZ, C. 2017. Non-linear differential equations and rotating disc electrodes: Padé approximation technique. Electrochimica acta, 243, pages 1-6. Held on OpenAIR [online]. Available from: https://openair.rgu.ac.uk

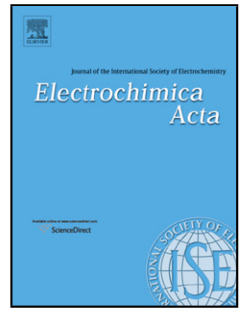

Title: Non-linear Differential Equations and Rotating Disc Electrodes: Padé approximationTechnique

Author: M. Chitra Devi L. Rajendran Ammar Bin Yousaf C. Fernandez

PII: S0013-4686(17)31044-7
DOI: http://dx.doi.org/doi:10.1016/j.electacta.2017.05.061
Reference: EA 29496

To appear in: *Electrochimica Acta*

Received date: 28-3-2017
Revised date: 9-5-2017
Accepted date: 10-5-2017

Please cite this article as: M. Chitra Devi, L. Rajendran, A.B. Yousaf, C. Fernandez, Non-linear Differential Equations and Rotating Disc Electrodes: Padé approximationTechnique, *Electrochimica Acta* (2017), http://dx.doi.org/10.1016/j.electacta.2017.05.061

HIGHLIGHTS

- Highly Non linear system of coupled equations are solved to describe the velocity and pressure components.
- The theoretical results enable to predict and optimize the performance of Rotating disk electrode.
- The analytical results are compared with the simulation result.

Non-linear Differential Equations and Rotating Disc Electrodes: Padé approximationTechnique

M. Chitra Devi[a], L. Rajendran[a], * Ammar Bin Yousaf[b], C. Fernandez[c]

[a] Department of Mathematics, Sethu Institute of Technology, Pulloor, Kariapatti-626115, Tamil Nadu, India

[b] Hefei National Lab for Physical Sciences at Microscale, University of Science and Technology of China, Hefei 230026, China.

[c] School of Pharmacy and Life Sciences, Robert Gordon University, AB107GJ, Aberdeen

* Corresponding author.

E-mail addresses: dr.rajendran.l@gamil.com, raj_sms@rediffmail.com
(L.Rajendran),chitradevi130492@gmail.com (M. Chitra Devi),
ammar@mail.ustc.edu.cn (A.B. Yousaf), c.fernandez@rgu.ac.uk (C. Fernandez).

Abstract

Rotating disc electrodes are preferred devices to analyze electrochemical reactions in electrochemical cellsand various rotating machinery such as fans, turbines, and centrifugal pumps. This model contains system of fully coupled and highly non-linear equations. This manuscript outlines the steady state solution of rotating disc flow coupled through the fluid viscosity, to the mass-concentration field of chemical species and heat transfer of power-law fluid over rotating disk. Furthermore, a simple analytical expression (Padé approximation) of velocity component/ self-similar velocity profiles is derived from the short and long distance expression. Our analytical results for all distance are compared with previous small and long distance and numerical solutions (Runge-Kutta method), which are in satisfactory agreement.

Keywords: Padé approximation, Mathematical modeling, Non-linear equations, Rotating disk electrodes.

1. Introduction

The system of second order non-linear equations in rotating disk electrodes and their studies arises in various contexts such as electrochemical cell [1]and flow and heat transfer process in fluids [2, 3] among others.Von Kármán swirling viscous flow [4] is a famous classical problem in fluid mechanics. The original problem raised by Von Kármán deals with the viscous flow induced by an infinite rotating disk where the fluid far from the disk is at rest. Steady laminar flows of viscous Newtonian fluid over an infinite rotating disk were studied originally by Von Kármán [4]. Von Kármán [4] proposed an elegant similarity transformation which reduces the Navier-Stokes equations to ordinary differential equations. The equations were then solved by the momentum integral method. Cochran [5] explained more accurate asymptotic series solution to Kármán's viscous pumping flow. Shevchuk [6] reported a new analytical solution with Nusselt number being specified as a boundary condition in the form of an arbitrary power-law function, and compared the results with experimental data. Levich *et al.* [7, 8] has solved the transient diffusion equation for the rotating disk electrode for the first time. Newman [9] obtained the uniform current density on a rotating disk electrode below the limiting current. Cahan *et al.* [10] developed a new method for mounting cylindrical samples for use as rotating disk electrodes which eliminates many of the problems associated with more conventional techniques.

Ariel [11] illustrated the flow of an elastico-viscous fluid near a rotating disk electrode and second-grade fluid [12]. In addition, perturbation solutions for small non-Newtonian fluid parameter and asymptotic analytical solutions for large parameter were also obtained. Attia [13] investigated the unsteady flow and heat transfer of Reiner-Rivlin fluid over a rotating disk by finite difference method as well as the effect of suction on the flow and heat transfer [14].In order to deal with the three-dimensional swirling flow over a rotating disk for power-law fluid, Mitschka [15] proposed a generalized Kármán similarity transformations. Chunying Ming *et al.* [3] solved the system of highly non-linear differential equations for the velocity, pressure and temperature field by an improved multi-shooting and Runge-Kutta method [16, 17].

Over the years, the importance of the fluid flow inside the electrochemical cell with rotating disk electrode have attracted a great interest [18, 19], however, at present this system has not been fully characterized. The early theoretical works dedicated to the hydrodynamic study of this system were presented by von Kármán [4] and Cochran [5].Two-dimensional axisymmetric numerical simulations were carried out[20] and compared with the fluid flow pattern calculated with the von Kármán [4] and Cochran [5] analytical expressions. There are significant differences in the extent of the electrochemical cell volume of the mathematical models reported in literature [1]. The entire cell volume was simulated in Mandin *et al.* [20] whereas in Dong *et al.* [21], only a small amount of liquid below a rotating disc ring electrode was considered. In these models only the electrode active face is in contact with the fluid.

The significance of the submerged electrode side wall was showed by means of two-dimensional numerical simulations of an electrochemical cell with a rotating cylinder electrode in Mandin *et al.* [22]. Dong *et al.*[21] carried out two-dimensional axisymmetric numerical simulations of a cell with a rotating disc electrode where the electrode is submerged into the electrolyte.Sorensen[23]reported that the system flow is governed by two parameters, the Reynolds number and the ratio of container height to disc radius. A comparison between the fluid flow pattern and that calculated with the model of von Kármán [4] and Cochran [5] is carried out.

Recently, Liao [24], developed a new analytical method for this non-linear problem using homotopy analysis method. The purpose of this communication is to derive approximate analytical expressions for the velocity component/ self-similar velocity profiles from small and long distance expressionsusing the Padé approximation method for all values of dimensionless distance.

2. Mathematical formulation of the problem

The equations for convective diffusion acquire their simplest form when the surface of a rotating disk serves as the reaction site. Von Karman [4] and Cochran [5] have solved the problem in which liquid is entrained by a rotating disk whose axis is perpendicular to its plane surface. The system of non-linear equations for convection diffusion process in rotating disk electrode are provided in Appendix A (Supplementary Information) for self-consistency, Von Karman [4].

The most famous approximate solution for small values of ξ are given by the following equations:

$$F(\xi) = a\xi - \frac{1}{2}\xi^2 - \frac{b}{3}\xi^3 + \cdots \tag{1}$$

$$G(\xi) = 1 + b\xi + \frac{a}{3}\xi^3 + \cdots \tag{2}$$

$$H(\xi) = -a\xi^2 + \frac{1}{3}\xi^3 + \frac{b}{6}\xi^4 + \cdots \tag{3}$$

where $a = 0.510$ and $b = -0.616$.

For large values of ξ, the dimensionless velocity components are:

$$F(\xi) = Ae^{-\alpha\xi} - \frac{(A^2+B^2)}{2\alpha^2}e^{-2\alpha\xi} + \frac{A(A^2+B^2)}{4\alpha^2}e^{-3\alpha\xi} + \cdots$$

(4) $G(\xi) = Be^{-\alpha\xi} - \dfrac{B(A^2+B^2)}{12\alpha^4}e^{-3\alpha\xi} + \cdots$

(5)

$$H(\xi) = -\alpha + \frac{2A}{\alpha}e^{-\alpha\xi} - \frac{(A^2+B^2)}{2\alpha^3}e^{-2\alpha\xi} + \frac{A(A^2+B^2)}{6\alpha^5}e^{-3\alpha\xi} + \cdots \tag{6}$$

where $A = 0.934$, $B = 1.208$ and $\alpha = 0.886$.

The above equation for large values of ξ can be rewritten as the following form:

$$F(\xi) \approx 0.00111 - \frac{0.10347}{\xi} + \frac{0.69753}{\xi^2} + \frac{1.3033}{\xi^3} - \frac{3.6398}{\xi^4} + \frac{1.9373}{\xi^5} \tag{7}$$

$$G(\xi) \approx -0.00025 + \frac{0.11152}{\xi} - \frac{2.8105}{\xi^2} + \frac{21.191}{\xi^3} - \frac{50.316}{\xi^4} + \frac{57.529}{\xi^5} - \frac{32.523}{\xi^6} + \frac{7.2882}{\xi^7} \tag{8}$$

$$H(\xi) \approx -0.88645 + \frac{0.2026}{\xi} - \frac{5.1647}{\xi^2} + \frac{39.982}{\xi^3} - \frac{101.09}{\xi^4} + \frac{122.82}{\xi^5} - \frac{73.611}{\xi^6} + \frac{17.495}{\xi^7} \tag{9}$$

3. Two-point Padé approximation

Our aim is to report a combined analytical result for the radial, tangential and the axial velocity component valid for all axial dimensionless distances, using mathematically rigorous procedures. Among several methods available for constructing a correct fractional approximation, the Padé approximation is one of the simplest and easy to implement. This is a rational function approximation to a power series obtained by matching the coefficients ofMaclaurin'sexpansionseries of the rational function with that of given power series [26]. Padé approximants are now employed normally in diverse contexts so as to overcome problems withslowly convergent or divergent power series expressions [27, 28].In view of the easy implementation of the algorithm, this technique is widely used in phase transitions and critical phenomena [29], virial equations of state for hard spheres and discs[30] and ultra-micro electrodes [31-33]. We constructeda rational function of order (5/5) such that the coefficient of Eqs. (A5) and (A6) are reproducible. The short and long distance expansions Eqs. (1-3) and Eqs. (4-6) can be merged in order to obtain a general form of rational function approximation $F(\xi), G(\xi)$ *and* $H(\xi)$valid for all distances, as follows:

$$Velocity = \frac{p_0 + p_1\xi + p_2\xi^2 + p_3\xi^3 + p_4\xi^4 + p_5\xi^5}{1 + q_1\xi + q_2\xi^2 + q_3\xi^3 + q_4\xi^4 + q_5\xi^5} \qquad (10)$$

where the Padé approximation coefficients p_0 to $p_5$andq_0 to q_5 are given in Table. A.The complete derivation of the above Padé approximant is given in the Appendix B-D (Supplementary Information). This (Eq. (10)) is a simplest closed-form of analytical approximation valid over the entire range of axial distance.Using Eqs. (A8) and (10) combined, we can obtain the pressure, as indicated by the equation below:

$$P(\xi) = \int_0^{\xi} \left(H''(\xi) - H(\xi)H'(\xi)\right)\, d\xi \qquad (11)$$

4. Numerical Simulation

Electrochemical simulations are one particular approach to understand the processes at electrodes [34-37].White *et al.* [38] solved the problem numerically by Newman technique [39]. Mathematical demonstration using Mathematica software for von Kármán swirling flow of RDE is created by Higgins and Binous [40]. Non-linear equations in rotating disk electrode (RDE) was solved by means of the self-adaptive method [25]. Bikash Sahool *et al.* [41] obtained the numerical solutions by adopting direct multiple shooting method for the fully coupled and highly non-linear system of differential equations, arising due to the steady Kármán flow and heat transfer of a viscous fluid in a porous medium. Recently, Ming *et al.* [3] solved the system of highly non-linear differential equations (A5-A7) by an improved multi-shooting method. Our analytical result for the velocity and pressure profiles are compared with numerical simulation. The comparison of analytical result obtained in this work with the numerical result obtained by multi shooting technique which is based on Runge-Kutta method is shown in Figure 1(a-d) in which satisfactory agreement is noted.Our analytical expression of velocity profiles (Padé approximation Eq. (20))is compared with small (Eqs. (1-3)) and long (Eqs. (4-6)) distance expressions in TableB and adequate agreement between the two approaches is noted.

5. Discussions

Von Kármán [4] gave the approximate solution of these equations based on the momentum integral method. Cochran [5] pointed out the errors contained in Kármán's solution and used a matching technique like Blasius method to give a solution more accurate than Kármán's one. Fettis [42] derived a new asymptotic expansion which can describe the entire flow and Benton [43] gave an asymptotic solution better than Cochran's solution using Fettis's method with only a trivial difference. Ariel derived the steady laminar flow of an elastico-viscous fluid near a rotating disk using perturbation technique [11].

For the first time Yang and Liao [24] obtained the analytical solution of von Kármán equations using the homotopy analysis method (HAM) [44, 45], as an infinite series Eq. (12). The homotopy series for the dimensionless axial velocity component converges slowly towards the exact solution of von Kármán equations. Hence, it is revealed that the series solution is not well suited to highly accurate computation of the diffusion–convection impedance for RDE. Recently, Liao [24] obtained the solution of the non-linear equation using homotopy analysis method as follows:

$$F(\xi)=\frac{-H'(\xi)}{2},\, H(\xi)\approx\sum_{k=0}^{M}\sum_{n=0}^{k+1}e^{-n\eta}\sum_{i=0}^{k+1}\alpha_{k,n}^{i}\eta^{i},\, G(\xi)\approx\sum_{k=0}^{M}\sum_{n=0}^{k+1}e^{-n\eta}\sum_{i=0}^{k+1}\beta_{k,n}^{i}\eta^{i} \qquad (12)$$

In the above solution it is very difficult to obtain the coefficients of η^i.However all the above mentioned solutions employed some numerical methods, such asanalytic, semi-numerical as well as essentially semi-ones. Thus, our analytical (Padé approximation) method is a simplest form which is valid for all values of ξ. The calculation of this method is free from computational software's, in which, we can calculate the Padé coefficients algebraically by doing simple steps.

Fig. 2 illustrates how the steady state radial, tangential and the axial velocity vary with ξ, respectively. Fig. 2(a), gives the distribution of radial velocity. It shows that the maximum value of radial velocity increases slightly with increasing power-law index. The thickness of the boundary layer decreases with the increasing power-law index [25]. It shows that the value of the radial velocity component rises initially and reaches the maximum value at $\xi = 0.8629$ and then decreases gradually until it reaches the steady state value. From the Fig. 2(b), it is evident that the value of the angular velocity component decrease from its initial value and reaches the steady state value zero at $\xi = \infty$. Maximum for $G(\xi)$ is 1.

Form the Fig.2(c), it is also observed that the axial velocity component always decreases when distance increases and reaches the steady state value at $\xi = \infty$. Maximum for $H(\xi)$is 0.The results demonstrated that increasing the axial distance increases the value of axial velocity and vice versa for tangential and total velocities.

6. Conclusions

Approximate analytical solutions to the system of non-linear differential equations are presented using Padé approximation method. A simple, straight forward and a new method of estimating the radial, tangential, axial velocity components have been reported. This analytical result will be useful to know the behaviour of the reaction system. In addition, this is a simple step solution for all distance to merge both the small and long distance expansions. For the first time, we have successfully reported a methodology which employs less time for analyzing small and large values of ξ separately, compared to previous studies. In addition, we can emphasized that our solution is highly specific and purely analytical due to the structure of the known solution. Furthermore, thePadé approximation coefficients in the series can be calculated algebraically. This proposed methodology does not require to use any numerical method to get such coefficients in contrast to Cochran's series solutions. Our analytical solutions are compared with numerical solutions and they are in very good agreement with the numerical simulation data.

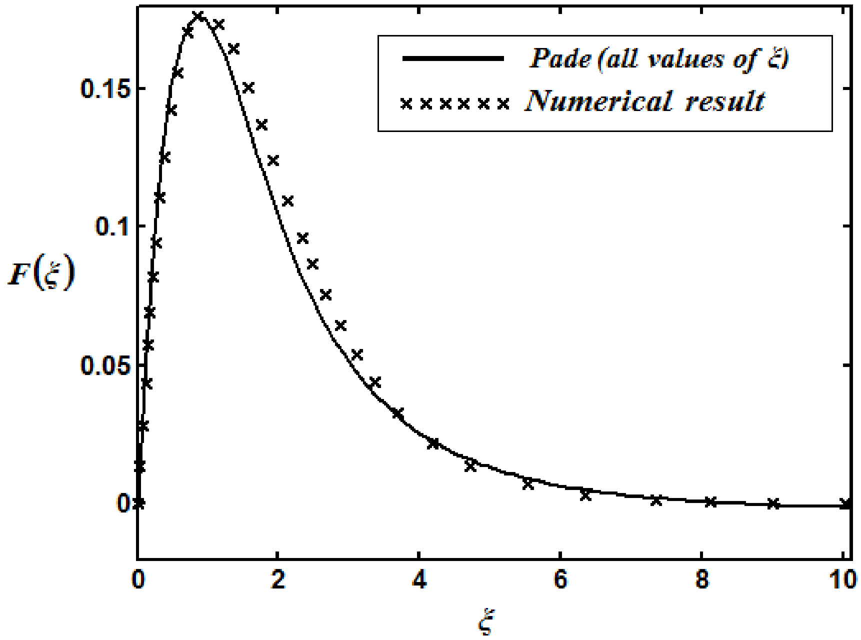

Fig. 1(a). Dimensionless radial velocity component $F(\xi)$ *versus* the dimensionless distance profile. The key to the graph: solid line represents Eq. (B10) and the dotted line represents the numerical [3].

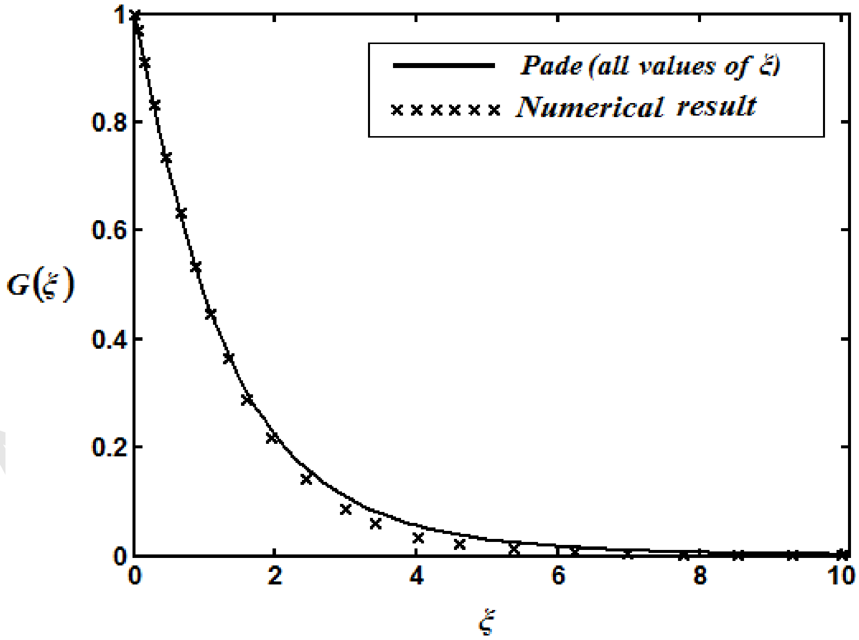

Fig. 1(b). Dimensionless tangential velocity component $G(\xi)$ *versus* thedimensionless distance profile. The key to the graph: solid line represents Eq. (C5) and the dotted line represents the numerical [3].

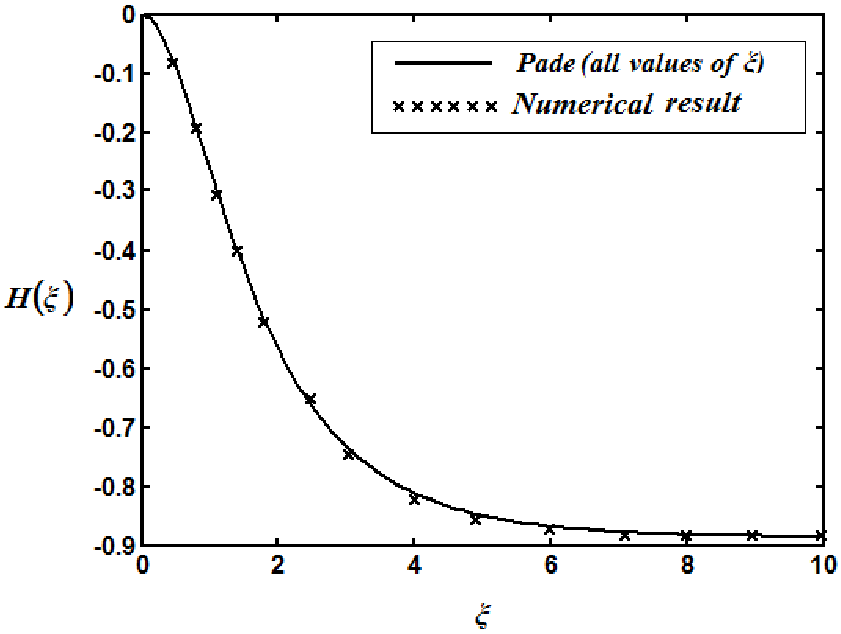

Fig. 1(c). Dimensionless axial velocity component $H(\xi)$ *versus* the dimensionless distance profile. The key to the graph: solid line represents Eq. (D5) and the dotted line represents the numerical [3].

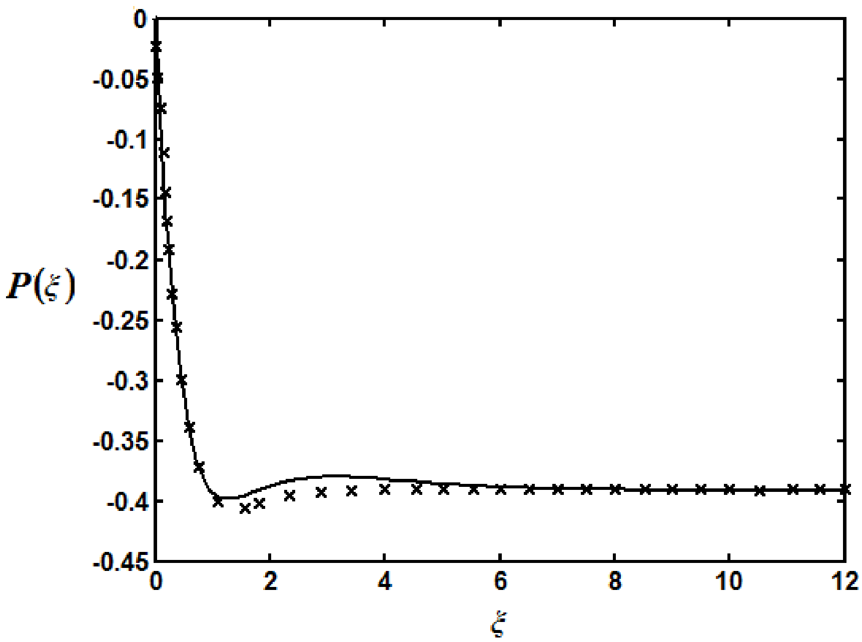

Fig.1 (d). Dimensionless pressure component $P(\xi)$ *versus* the dimensionless distance profile. The key to the graph: solid line represents Eq. (11) and the dotted line represents the numerical [3].

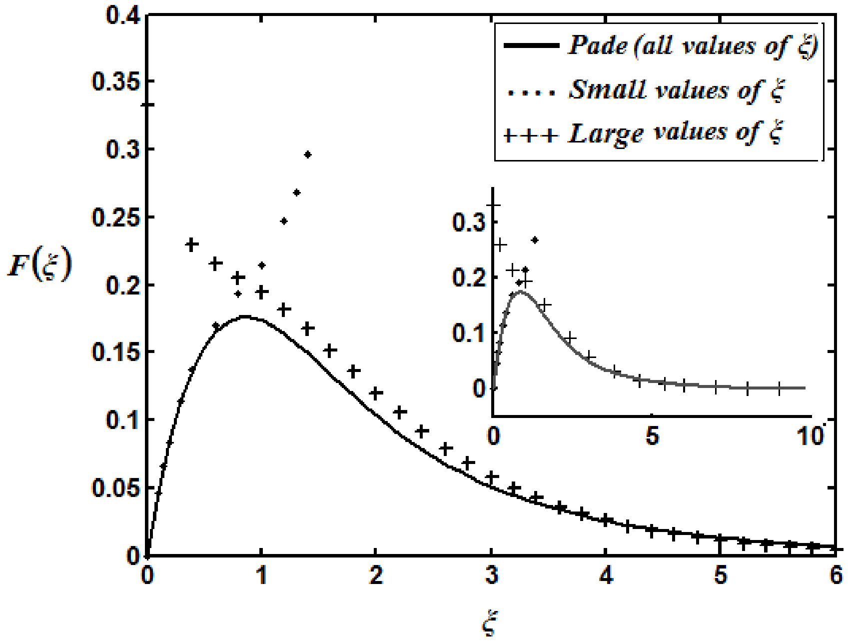

Fig. 2(a). Comparison of our radial velocity component $F(\xi)$ (Padé approximation Eq. (B10)) *versus* the dimensionless distance ξ with small (Eq. (1)) and long solution (Eq. (7)).

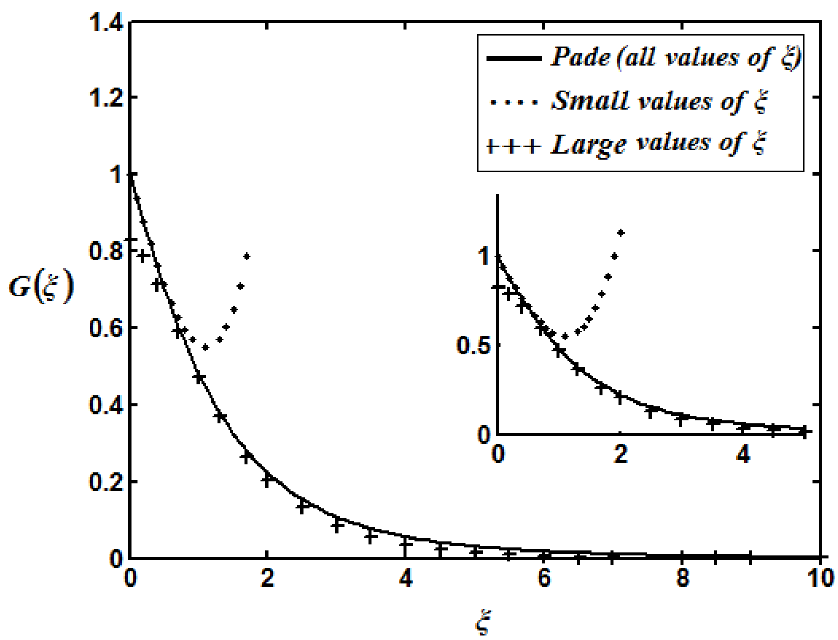

Fig. 2(b). Comparison of our tangential velocity component $G(\xi)$ (Padé approximation Eq. (C5)) *versus* the dimensionless distance ξ with small (Eq. (2)) and long solution (Eq. (8)).

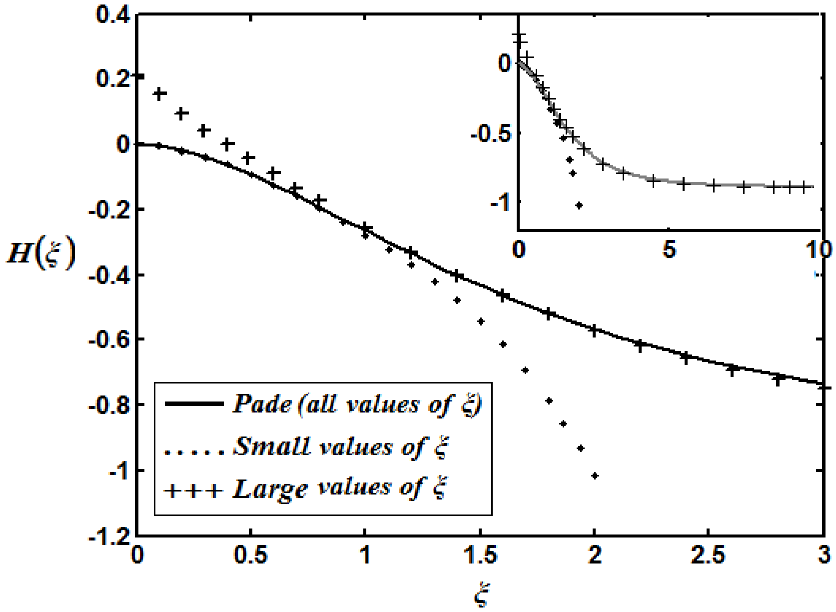

Fig. 2(c). Comparison of our axial velocity component $H(\xi)$ (Padé approximation Eq. (D5)) *versus* the dimensionless distance ξ with small (Eq. (3)) and long solution (Eq. (9)).

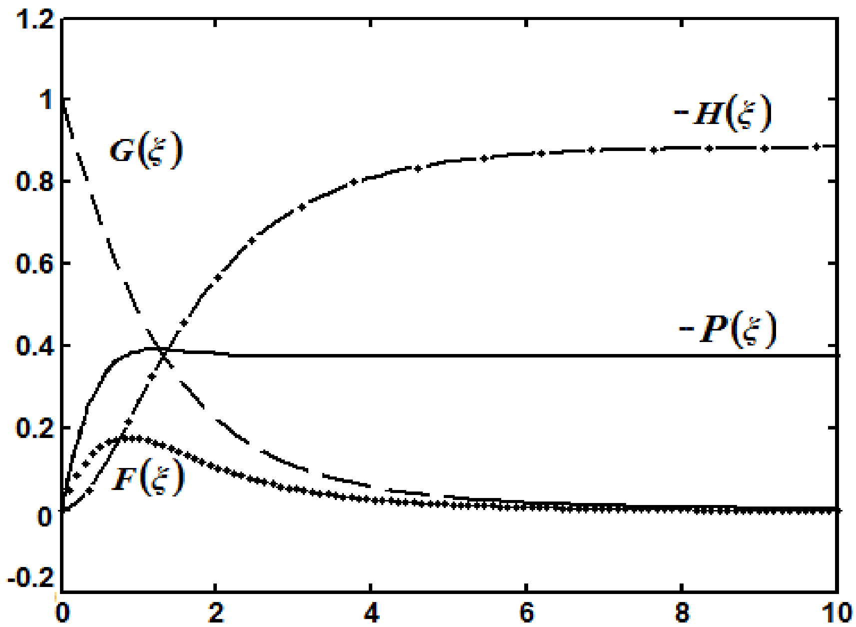

Fig. 3. Plot for analytical solution of velocity and pressure using Eqs. (10-11).

Table. A. Numerical value of Padé approximation coefficients for $F(\xi)$, $G(\xi)$ and $H(\xi)$

Padé Coefficients	$F(\xi)$	$G(\xi)$	$H(\xi)$
p_0	*0*	*1*	*0*
p_1	*0.51000*	*0.04812*	*0*
p_2	*0.33506*	*-0.01933*	*0.51000*
p_3	9.95187×10^{-3}	*0.00106*	*-0.10187*
p_4	-7.31242×10^{-3}	*0*	*-0.02892*
p_5	8.32389×10^{-5}	*0*	*0*
q_1	*1.63737*	*0.66412*	*0.85335*
q_2	*1.22223*	*0.38977*	*0.41316*
q_3	*0.52480*	*0.07116*	*0.12238*
q_4	*0.41588*	*0.00966*	*0.03263*
q_5	*0.07513*	*0*	*0*

Table. B. Comparison of approximate analytical expression (Padé approximation Eq. (20)) of velocity profiles $F(\xi)$, $G(\xi)$ and $H(\xi)$ with small and long distance expressions

Dimensionless Distance ξ	$F(\xi)$ **Radial velocity**					$G(\xi)$ **Tangential velocity**					$H(\xi)$ **Axial velocity**				
	Eq.(20) or Eq.(B10) Padé	**Eq.(1) Small ξ**	**Eq.(4) Large ξ**	**Error percentage**		**Eq.(20) or Eq.(C5) Padé**	**Eq.(2) Small ξ**	**Eq.(5) Large ξ**	**Error percentage**		**Eq.(20) or Eq.(D5) Padé**	**Eq.(3) Small ξ**	**Eq.(6) Large ξ**	**Error percentage**	
0.000	*0*	*0*		*0*		*1*	*1*		*0*		*0*	*0*		*0*	
0.001	*0.00*	*0.00*		*0*		*1.00*	*1.00*		*0*		*0.00*	*0.00*		*0*	
0.05	*0.02*	*0.02*		*0*		*0.97*	*0.97*		*0*		*0.00*	*0.00*		*0*	
0.1	*0.05*	*0.05*		*0*		*0.94*	*0.94*		*0*		*0.00*	*0.00*		*0*	
0.2	*0.08*	*0.08*		*0*		*0.88*	*0.88*		*0*		*-0.02*	*-0.02*		*0*	
0.4	*0.14*	*0.14*		*1*		*0.76*	*0.76*		*0*		*-0.06*	*-0.06*		*0*	
0.6	*0.16*	*0.17*		*3*		*0.66*	*0.67*		*1.5*		*-0.12*	*-0.12*		*0*	
0.8	*0.18*	*0.19*		*10*		*0.56*	*0.59*	*0.55*	*1.7*	*1*	*-0.19*	*-0.20*	*-0.18*	*5*	*5*
1	*0.17*	*0.22*	*0.19*	*24*	*12*	*0.48*		*0.47*		*2*	*-0.26*		*-0.26*		*0*
2	*0.10*		*0.12*		*20*	*0.22*		*0.20*		*9*	*-0.57*		*-0.57*		*0*
3	*0.05*		*0.06*		*20*	*0.10*		*0.08*		*20*	*-0.73*		*-0.75*		*2*
4	*0.03*		*0.03*		*0*	*0.05*		*0.04*		*20*	*-0.81*		*-0.83*		*2*
5	*0.01*		*0.01*		*0*	*0.03*		*0.03*		*0*	*-0.85*		*-0.86*		*1*
10	*0.00*		*0.00*		*0*	*0.00*		*0.00*		*0*	*-0.89*		*-0.89*		*0*
∞	*0*		*0*		*0*	*0*		*0*		*0*	$-0.886\,(=-\alpha)$		$-0.886\,(=-\alpha)$		*0*

Acknowledgement

This work was supported by the Department of Science and Technology, SERB-DST (EMR/2015/002279) Government of India. Also the authors thanks to Mr. S. Mohamed Jaleel, the Chairman and Dr. A. Senthil Kumar, the Principal and Dr. P. G. Jansi Rani, Head of the Department of Mathematics, Sethu Institute of Technology, Kariapatti, India for their constant encouragement.

Nomenclature

u	radial velocity component (m/s)
v	tangential or angular velocity component (m/s)
w	axial velocity component (m/s)
r	radial coordinate (m)
z	normal or axial coordinate (m)
p	pressure (N/m)
ρ	density of the fluid (kg/m^3)
ν	kinematic viscosity of the fluid
ω	electrode rotation speed
F	self-similar radial velocity or dimensionless radial velocity component
G	self-similar tangential velocity or dimensionless angular velocity component
H	self-similar axial velocity or dimensionless axial velocity component
$p_i,\ q_i$	Padé approximation co-efficient

References

[1] A. Cesar, Real-Ramirez, Ralul Miranda-Tello, F. Luis, Hoyos –Reues and I. Jwsus, Gonzalez-Trejo, Hydrodynamic characterization of an electrochemical cell with rotating disc electrode: a three-dimensional biphasic model, International Journal of Chemical Reactor Engineering, 8 (2010) 1-37.

[2] ShuoXun, Jinhu Zhao, Liancun Zheng, Xuehui Chen, Xinxin Zhang, Flow and heat transfer of Ostwald-de Waele fluid over a variable thickness rotating disk with index decreasing, International Journal of Heat and Mass Transfer, 103 (2016) 1214–1224.

[3] Chunying Ming, Liancun Zheng, Xinxin Zhang, Fawang Liu, Vo Anh, Flow and heat transfer of power-law fluid over a rotating disk when generalized diffusion, International Communication in Heat and Mass Transfer, 79 (2016) 81-88.

[4] T. Von Kármán, Überlaminare und turbulentereibung, Journal of Applied Mathematics and Mechanics, 1 (1921) 233-252.

[5] W. G. Cochran, The flow due to a rotating disc, Proceedings of the Cambridge Philosophical Society, 30 (1934) 365-375.

[6] I.V. Shevchuk, A new type of the boundary condition allowing analytical solution of the thermal boundary layer equation, Int. J. Therm. Sci, 44 (2005) 374–381.

[7] B. Levich, The Theory of Concentration Polarization, ActaPhysicochim. URSS, 17 (1942) 257–307.

[8] B. Levich, Physicochemical Hydrodynamics, Prentice Hall, Englewood Cliffs, 1962.

[9] J. Newman, Current Distribution on a Rotating Disk below the Limiting Current, Journal of Electrochemical Society, 113 (1966)1235-1241.

[10] B.D. Cahan and H.M. Villullas, The hanging meniscus rotating disk (HMRD), Journal of Electroanalytical Chemistry, 307 (1991) 263-268.

[11] P.D. Ariel, On the flow of an elastico-viscous fluid near a rotating disk, J. Comput. Appl. Math, 154 (2003) 1–25.

[12] P.D. Ariel, Computation of a second grade fluid near a rotating disk, Int. J. Eng. Sci, 35 (4) (1997) 1335–1357.

[13] H.A. Attia, Unsteady flow of a non-Newtonian fluid above a rotating disk with heat transfer, Int. J. Heat Mass Transfer, 46 (2003) 2695–2700.

[14] H.A. Attia, Rotating disk flow and heat transfer through a porous medium of a non-

Newtonian fluid with suction and injection, Commun. Non-linear Sci. Numer. Simul, 13 (2008) 1571–1580.

[15] P. Mitschka, Nicht-Newtonsche Flüssigkeiten II. Drehströmung Ostwald-de Waelescher Nicht-Newtonscher Flüssigkeiten, Coll. Czech. Chem. Comm, 29 (1964) 2892–2905.

[16] Fengxia Wang, Bifurcations of nonlinear normal modes via the configuration domain and the time domain shooting methods, Communications in Nonlinear Science and Numerical Simulation, 20(2)(2015) 614-628.

[17] F. Capuano, G. Coppola, L. Rández, L. de Luca, Explicit Runge–Kutta schemes for incompressible flow with improved energy-conservation properties, Journal of Computational Physics, 328(1) (2017) 86-94.

[18] A. Bard, and R. Faulkner (2001). Electrochemical methods: Fundamentals and applications. New York, USA, Wiley Interscience.

[19] Q. Dong, and S. Santhanagopalan, A comparison of numerical solutions for the fluid motion generated by a rotating disk electrode, Journal of the Electrochemical Society, 155 (9) (2008) B963-B968.

[20] P. Mandin, and T. Pauporte, Modelling and numerical simulation of hydro dynamical processes in a confined rotating electrode configuration, Journal of Electroanalytical Chemistry, 565(2) (2004) 159-173.

[21] Q. Dong, and S. Santhanagopalan, Simulation of the oxygen reduction reaction at an RDE in 0.5 m H2SO4 including an adsorption mechanism, Journal of the Electrochemical Society, 154(9) (2007) A888-A899.

[22] P. Mandin, C. Fabian, et al, Importance of the density gradient effects in modelling electro deposition process at a rotating cylinder electrode, Electrochimica Acta 51(9) (2006) 4067-4079.

[23] J. N. Sorensen, and I. Naumov, Experimental investigation of three dimensional flow instabilities in a rotating lid-driven cavity, Experiments in Fluids, 41(3) (2006) 425-440.

[24] Cheng Yang, Shijun Liao, On the explicit, purely analytic solution of Von Kármán swirling viscous flow, Communication in Non-linear Science and Numerical Simulation, 11(2006)83-93.

[25] J.P. Diard, C. Montella, Re-examination of the diffusion–convection impedance for a uniformly accessible rotating disk. Computation and accuracy, Journal of Electroanalytical Chemistry, 742 (2015) 37–46.

[26] G.A. Baker, P. Greaves-Morries, in: G.C. Rotta (Ed.), Padé Approximations. Part II. Encyclopaedia of Mathematics, vol. 3, Addison-Wesley, Reading, MA, 1981 (Chapter 1).

[27] C. Ahmed Basha, M.V. Sangaranarayanan, On the evaluation of the current function in linear sweep voltammetry, J. Electroanal. Chem., 261 (1989) 431.

[28] V. Rajendran, Ph.D. Thesis, Alagappa University, Karaikudi (1998).

[29] D.D. Gaunt, A.J. Guttmann, in: C. Domb, M.S. Green (Eds.), Phase Transitions and Critical Phenomena, Academic Press, New York, 1981.

[30] K.W. Kratky, Equation of state of a hard disk fluid. I. The virial expansion, J. Chem. Phys. 69 (1978) 2251.

[31] L. Rajendran and M.V. Sangaranarayanan, Diffusion at ultra-micro disc electrodes: chronoamperic current for steady state EC' reaction using scattering analog techniques, Journal of Physical Chemistry. B, 103 (1999) 1518-1524.

[32] L. Rajendran, Padé approximation for ECE and DISP processes at channel electrodes, Electrochemistry Communication, 2 (2000) 186-189.

[33] L. Rajendran, Analysis of non-steady state current at hemispheroidal ultra-micro electrodes, Electrochemistry Communication, 2 (2000) 531-534.

[34] B. Speiser, A.J. in Bard, Rubinstein, I. (Ed.), Electroanalytical Chemistry, Marcel Dekker, Newyorkvol, 19 (1996) 1 – 108.

[35] D. Britz, Digital Simulations in Electrochemistry, Second, revised and extended edition, Springer-Verlag, Berlin, 1988.

[36] L. K. Bieniasz and D. Britz, Recent Developments in Digital Simulation of Electroanalytical Experiments (Review), Pol. J. Chem., vol. 78 (2004) 1195.

[37] R.G. Compton, E. Laborda, K. R. Ward, Understanding Voltammetry - Simulation of Electrode Processes World Scientific (2014).

[38] R. White, C.M. Mohr, J. Newman, J. Electrochem. Soc. 123 (1976) 383.

[39] J. Newman, in: A.J. Bard (Ed.), Electroanalytical Chemistry, vol. 6, Marcel Dekker Inc., New York, 1973, p. 187.

[40] B.G. Higgins, H. Binous. <http://demonstrations.Wolfram.com/Steady Flow over A Rotating Disk Von Kármán Swirling Flow/>.

[41] Bikash Sahoo, Sébastien Poncet, and Fotini Labropulu, Effects of slip on the Von Kármán swirling flow and heat transfer in a porous medium, Transactions of the Canadian Society for Mechanical Engineering, 39(2) (2015) 357-366.

[42] Fettis, HE. On the integration of a class of differential equations occurring in boundary layer and other hydrodynamic problems, In: Proceeding of 4thMidwesten Conference on Fluid Mechanics, Purdue. 1955.

[43] Bendon Edward R. On the flow due to a rotating disk, J Fluid Mech, 24 (1966), 781-800.

[44] S. Liao, Beyond Perturbation: Introduction to Homotopy Analysis Method, Chapman& Hall/CRC Press, Boca Raton, 2003.

[45] S. J. Liao, Notes on the homotopy analysis method: some definitions and theorems. Commun. Non-linear Sci. Numer. Simul. 14(4) (2009) 983-997.

Figure Captions

Fig. 1(a). Dimensionless radial velocity component $F(\xi)$ *versus* the dimensionless distance profile. The key to the graph: solid line represents Eq. (B10) and the dotted line represents the numerical [3].

Fig. 1(b). Dimensionless tangential velocity component $G(\xi)$ *versus* the dimensionless distance profile. The key to the graph: solid line represents Eq. (C5) and the dotted line represents the numerical [3].

Fig. 1(c). Dimensionless axial velocity component $H(\xi)$ *versus* the dimensionless distance profile. The key to the graph: solid line represents Eq. (D5) and the dotted line represents the numerical [3].

Fig. 1(d). Dimensionless pressure component $P(\xi)$ *versus* the dimensionless distance profile. The key to the graph: solid line represents Eq. (11) and the dotted line represents the numerical [3].

Fig. 2(a). Comparison of our radial velocity component $F(\xi)$ (Padé approximation Eq. (B10)) *versus* the dimensionless distance ξ with small (Eq. (1)) and long solution (Eq. (7)).

Fig. 2(b). Comparison of our tangential velocity component $G(\xi)$ (Padé approximation Eq. (C5)) *versus* the dimensionless distance ξ with small (Eq. (2)) and long solution (Eq. (8)).

Fig. 2(c). Comparison of our axial velocity component $H(\xi)$ (Padé approximation Eq. (D5)) *versus* the dimensionless distance ξ with small (Eq. (3)) and long solution (Eq. (9)).

Fig. 3. Plot for analytical solution of velocity and pressure using Eqs. (10-11).